Sustainable aviation fuel production using in-situ hydrogen supply via aqueous phase reforming: A techno-economic and life-cycle greenhouse gas emissions assessment

Journal of Cleaner Production 418 (2023) 138141

Contents lists available at ScienceDirect

Journal of Cleaner Production

journal homepage: www.elsevier.com/locate/jclepro

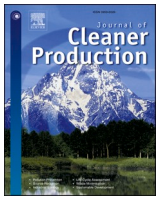

Sustainable aviation fuel production using in-situ hydrogen supply via aqueous phase reforming: A techno-economic and life-cycle greenhouse gas emissions assessment

Giuseppe Pipitone *, Giulia Zoppi, Raffaele Pirone, Samir Bensaid

Department of Applied Science and Technology, Politecnico di Torino, Corso Duca degli Abruzzi 24, 10129, Turin, Italy

ARTICLE INFO

Handling Editor: Panos Seferlis

Keywords:
Aqueous phase reforming
GHG reduction
Hydrogenated vegetable oil
Sustainable aviation fuel
Techno-economic assessment

ABSTRACT

Sustainable aviation fuel (SAF) production is one of the strategies to guarantee an environmental-friendly development of the aviation sector. This work evaluates the technical, economic and environmental feasibility of obtaining SAFs by hydrogenation of vegetable oils thanks to in-situ hydrogen production via aqueous phase reforming (APR) of glycerol by-product. The novel implementation of APR would avoid the environmental burden of conventional fossil-derived hydrogen production, as well as intermittency and storage issues related to the use of RES-based (renewable energy sources) electrolysers. The conceptual design of a conventional and advanced (APR-aided) biorefinery was performed, considering a standard plant capacity equal to 180 ktonne/y of palm oil. For the advanced scenario, the feed underwent hydrolysis into glycerol and fatty acids; hence, the former was subjected to APR to provide hydrogen, which was further used in the hydrotreatment reactor where the fatty acids were deoxygenated. The techno-economic results showed that APR implementation led to a slight increase of the fixed capital investment by 6.6% compared to the conventional one, while direct manufacturing costs decreased by 22%. In order to get a 10% internal rate of return, the minimum fuel selling price was found equal to 1.84 $/kg, which is 17% lower than the one derived from conventional configurations (2.20 $/kg). The life-cycle GHG emission assessment showed that the carbon footprint of the advanced scenario was equal to ca. 12 g CO_2/MJ_{SAF}, i.e., 54% lower than the conventional one (considering an energy-based allocation). The sensitivity analysis pointed out that the cost of the feedstock, SAF yield and the chosen plant size are keys parameters for the marketability of this biorefinery, while the energy price has a negligible impact; moreover, the source of hydrogen has significant consequences on the environmental footprint of the plant. Finally, possible uncertainties for both scenarios were undertaken via Monte Carlo simulations.

1. Introduction

The aviation sector is responsible for approximately 2% of anthropogenic greenhouse gas emissions worldwide (Terrenoire et al., 2019). With air transportation predicted to triplicate in 2050 with respect to the beginning of this century, there is a need for solutions for its decarbonization, and biofuels are seen as a potential option in this regard (Bhutto et al., 2016). Nowadays, bioethanol and biodiesel are the most used alternative fuels to fossil ones. In addition, hydrogenated vegetable oils are increasing their volume due to their similarities with crude processing, complete blending with conventional fuels, better quality of the final product, etc. (Vásquez et al., 2017). The path for the sustainable production of transport fuels is pushed particularly by the aviation sector, where strict quality requirements (e.g., low freezing point, absence of oxygenates and heteroatoms) are demanded and alternative mitigation strategies (such as electrification) are still challenging (Heyne et al., 2021).

In this context, the deployment of sustainable aviation fuels (SAFs) can play a critical role, gradually substituting fossil kerosene thanks to the introduction of new agreements, such as CORSIA (Carbon Offset and Reduction Scheme for International Aviation) (Ng et al., 2021). They can be produced following different routes, which are nowadays at diverse technology readiness level: Fischer-Tropsch synthesis, synthesized iso-paraffinic, alcohol to jet, catalytic hydrothermolysis and hydroprocessed esters and fatty acids (Shahriar and Khanal, 2022). In addition, electrofuels, battery-based systems and hydrogen are being investigated as developing substitute energy sources (Su-ungkavatin

* Corresponding author.
E-mail address: giuseppe.pipitone@polito.it (G. Pipitone).

https://doi.org/10.1016/j.jclepro.2023.138141
Received 5 May 2023; Received in revised form 13 July 2023; Accepted 16 July 2023
Available online 17 July 2023

Abbreviation list

APR	Aqueous phase reforming
ASTM	American society for testing and materials
BFD	Block flow diagram
CBM	Bare module cost
CEPCI	Chemical engineering plant cost index
CF	Cash flow
COL	Operating labor costs
COM	Manufacturing costs
COMd	Manufacturing costs without depreciation
CORSIA	Carbon offset and reduction scheme for international aviation
CP	Purchased cost
CRM	Raw materials cost
CUT	Utilities cost
CWT	Waste treatment cost
DCF	Discounted cash flow
DeCO	Decarbonylation
$DeCO_2$	Decarboxylation
DMC	Direct manufacturing costs
DR	Discount rate
EGM	European grid mix
FBM	Bare module cost factor
FCI	Fixed capital investment
FMC	Fixed manufacturing costs
GE	General expenses
GHG	Greenhouse gas
GWP	Global warming potential
HDO	Hydrodeoxygenation
HEFA	Hydroprocessed esters and fatty acids
HI/HC	Hydroisomerization/Hydrocracking
HRJ	Hydroprocessed renewable jet
LCA	Life-cycle assessment
LHV	Lower heating value
MFSP	Minimum fuel selling price
NPV	Net present value
POC	Palm oil cost
PSA	Pressure swing adsorption
R&D	Research and development
RES	Renewable energy sources
SAF	Sustainable aviation fuel
TCI	Total capital investment
TEA	Techno-economic assessment
WC	Working capital
WHSV	Weight hourly space velocity

et al., 2023). Independently from the chosen pathway, SAFs require several characteristics for being effectively implemented, such as being competitive both technically, economically, and environmentally, in addition to being easily available. In this sense, determining the production cost is crucial for evaluating its commercial applicability (Martinez-Hernandez et al., 2019).

Eni and Honeywell UOP commercialized for the first time a technology (known as Ecofining™) able to derive SAFs starting from biomass via hydroprocessing (Bashir et al., 2022). The ASTM-certified output from this process is known as hydroprocessed renewable jet (HRJ) or hydroprocessed esters and fatty acids (HEFA) and can be used up to 50% in blend with conventional jet fuel without any prior modification in the engines. It is worth noting that such fuels have a higher energy density with respect to the ones derived from alternative pathways cited above, and could be theoretically used without blending (Wei et al., 2019). While it is difficult comparing the different routes towards SAF under the financial point of view due to the absence of a standard methodology, it was showed that this technology has typically the lowest minimum selling price (Martinez-Valencia et al., 2021).

The conventional block flow diagram for HRJ production is depicted in Fig. 1. It foresees a series of two reactors. In the first one, the feedstock is put in contact with hydrogen and a heterogeneous catalyst: within this reactor, the double bonds present in the triglycerides are firstly saturated; afterwards, the ester is cleaved to propane and three free fatty acids; finally, they are deoxygenated via three possible reaction mechanisms (please refer to paragraph 3.1 for further details) to produce n-alkanes (Gosselink et al., 2013). Since alkanes do not meet jet fuel requirements, an upgrade is performed in a second reactor, where the mixture of paraffines is isomerized and cracked in the presence of hydrogen to reach the jet fuel requirements (e.g., flash point and cold flow properties). During this reaction step, also other products obtained, such as naphtha and diesel. This multicomponent stream is hence finally separated thanks to a distillation column to obtain the desired product, as well as lighter and heavier by-products.

Different feedstocks were evaluated depending on peculiar characteristics, such as jatropha due to the high oil yields (Wang, 2016), rapeseed/algae oils or low-input oilseeds (camelina, carinata, and used-cooking oil) (Chu et al., 2017; Shila and Johnson, 2021; Tao et al., 2017).

One drawback highlighted in this scenario is the high consumption of hydrogen for the saturation/deoxygenation reactions, which is an environmental and economic burden for the technology (Sadhukhan and Sen, 2021). In the available literature, hydrogen is commonly considered as derived from steam methane reforming, in accordance with actual hydrogen production method. However, other possibilities are being investigated. One option is related to decarboxylation/decarbonylation reactions, for which the hydrogen demand decreases (Kubičková et al., 2005). Scaldaferri et al. developed a niobium phosphate catalyst able to deoxygenate soy oil under inert atmosphere (Scaldaferri and Pasa, 2019). Zakir Hossain and co-workers used oleic acid as model compound to perform its deoxygenation coupling decarboxylation and in situ hydrogen production with activated carbon (Hossain et al., 2018). Some works present in literature suggest alternative methods, including catalytic transfer hydrogenation,

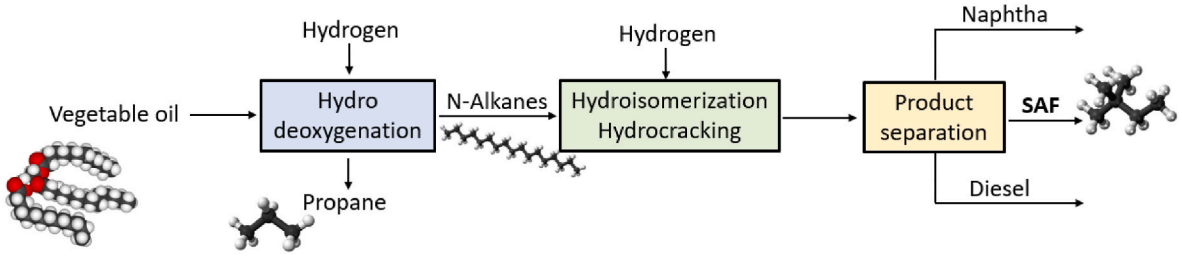

Fig. 1. Block flow diagram of a conventional SAF production plant (HEFA technology) used as benchmark in this study.

which involves using a suitable solvent or molecule (in the liquid phase) as a hydrogen-donor (Barbera et al., 2020; Hwang et al., 2016; Zhong et al., 2019).

To achieve a completely renewable production of aviation fuels, it is self-evident that the used hydrogen must not come from fossil sources. Currently, the most available renewable hydrogen technology is water electrolysis; however, its costs are still too high and need significant improvements. Zech et al. proposed a solution using the power-to-gas concept to produce green hydrogen, but production costs increased by 34% (Zech et al., 2018).

An alternative approach for in-situ hydrogen production is exploiting the aqueous phase reforming (APR) reaction. APR was firstly studied by Dumesic and coworkers for its possibility to produce H_2 from biomass-derived compounds under milder reaction conditions (220–270 °C, 30–60 bar) compared to conventional fossil-based steam reforming (Equation (1) in the case of glycerol APR) (Cortright et al., 2002). APR presents several advantages since it avoids the need to vaporize water, reducing the energy requirement, and generates a CO-poor gas phase in one single reactor, thanks to the favorable equilibrium for the water gas shift reaction.

$$C_3H_8O_3 + 3H_2O \rightarrow 3CO_2 + 7H_2 \quad (1)$$

Fig. 2 shows how this reaction could be exploited for the SAF production.

The triglycerides may firstly undergo an hydrolysis step (Costa et al., 2020). Such reaction breaks the ester bonds, allowing to obtain free fatty acids and glycerol. As a matter of fact, the latter is a suitable substrate for the aqueous phase reforming, and hence for hydrogen production, as reported in several works (Fasolini et al., 2019). Consequently, it could replace, at least partially, the necessary external hydrogen for the deoxygenation and isomerization/cracking of the fatty acids.

Dominguez-Barroso et al. showed that it was possible to deoxygenate sunflower oil under inert and hydrothermal conditions using a Pd-based catalyst thanks to the fact that glycerol, a by-product of triglyceride hydrolysis, underwent APR and led to hydrogen in the reaction environment (Domínguez-Barroso et al., 2016). The simultaneous hydrolysis-hydrogenation was also investigated successively by several authors, evaluating different catalytic systems to maximize the production of deoxygenated hydrocarbons (Crisostomo et al., 2021; Domínguez-Barroso et al., 2019; Kouzu et al., 2021). However, under an industrial point of view, it could be meaningful separating these steps in different reactions where the reaction conditions are optimized, in order to maximize the fuel production. This is a promising alternative to green hydrogen which, aiming to exploit fully renewable electricity, would require heavy investments for dealing with fluctuations and storages issues (Salkuti, 2022).

Starting from this knowledge, this work provides a unique perspective by specifically focusing on the implementation of in-situ hydrogen production in the biorefinery by glycerol APR, and its impact on the economic and environmental aspects of SAFs production with respect to the actual HEFA process concept. Firstly, a conceptual design of the conventional and advanced biorefinery was performed; afterwards, the minimum fuel selling price (MFSP) and GHG emissions were derived for the two scenarios, identifying the variables with the highest impact on both indicators. Starting from this information, a sensitivity analysis was carried out changing singularly the most important variables (e.g., plant size, fixed capital investment, feed price etc.). Particular attention was finally paid to the uncertainties related to the low technology readiness level of this technology by performing Monte Carlo simulations.

2. Methodology

2.1. Process design

Two scenarios are presented in this work, whose plant capacity was set at 180 ktonne/y of palm oil, in accordance with the size of typical vegetable oil-based biorefineries (Shahriar and Khanal, 2022). The composition of palm oil was assumed as follows: 45.8 wt% tripalmitin, 4.3 wt% tristearin, 39.3 wt% triolein, 10 wt% trilinolein (Issariyakul and Dalai, 2014). Mass and energy balances for both scenarios were modelled in Microsoft Excel, using information previously reported by the literature regarding conversion of the feedstock, products yield, and so on. 1-octene, dodecane and heptadecane were used as representative compounds of, respectively, naphtha, kerosene and diesel for energy balance purposes and the design of the heat exchanger network.

The block flow diagram (BFD) of the conventional scenario was reported in Fig. 1. After heating, pressurization and mixing with a hydrogen stream (2.7 wt% in agreement with (Han et al., 2013)), palm oil is firstly hydrotreated, meaning that triglycerides are converted into linear, oxygen-free paraffins. Table 1 depicts the reactions involved in the hydrodeoxygenation (HDO) reactor, starting from triolein (analogously for other triglycerides). References on the thermal effects reported therein can be found and/or derived from (Jęczmionek and Porzycka-Semczuk, 2014).

It is assumed that the double bonds are fully saturated (a), free fatty acids and propane are formed due to hydrogen-assisted cleavage of triglycerides (b), and oxygen is removed through three parallel reactions which are HDO, decarbonylation (DeCO) and decarboxylation ($DeCO_2$) (c1-3). The extent of such reactions was derived from the work of Chu et al. (2017). In accordance with (Veriansyah et al., 2012), methanation was excluded in this reactor. Propane (and other light alkanes) can be sold as fuel gas, taking into consideration that its energetic value is similar to the one of natural gas.

In the second reactor, hydrocracking and hydroisomerization occur to obtain a jet fuel with suitable properties (i.e., boiling point in the 140–250 °C range, high flash point, good cold flow properties etc.). In this reactor, apart from desired reactions where jet fuel is obtained (d), undesired small alkanes can be produced as well.

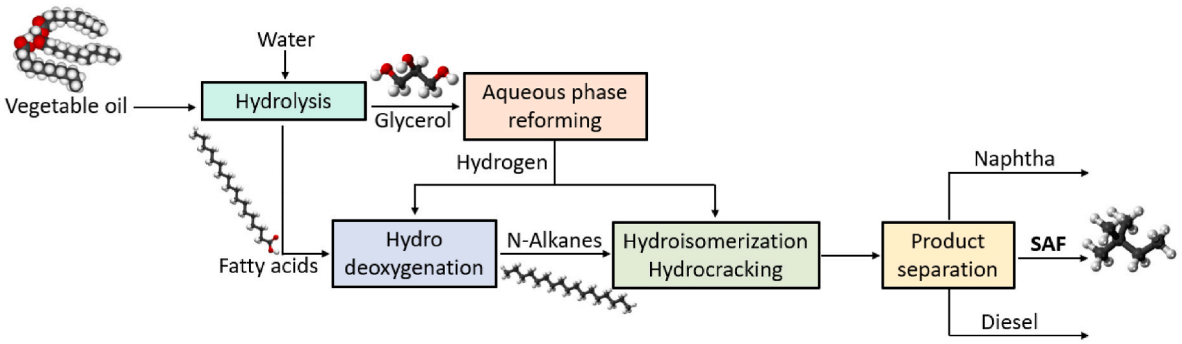

Fig. 2. Block flow diagram of the advanced SAF production plant proposed in this study, with the employment of two new steps (hydrolysis and aqueous phase reforming).

Table 1
List of reactors employed in the conventional scenario. An example of the reactions carried out in each unit is also reported, together with the extent of reaction and enthalpy.

Conventional scenario				Reference
Reactor	Reaction	Extent of reaction	Reaction enthalpy	
Hydrodeoxygenation	a) triolein +3 H_2 → tristearin	100%	−303 kJ/mol	Gosselink et al. (2013)
	b) tristearin +3 H_2 → 3 stearic acid + propane	100%	+251 kJ/mol	Gosselink et al. (2013)
	c1) stearic acid + 3 H_2 → octadecane + 2 H_2O	29%	−129.6 kJ/mol	Chu et al. (2017)
	c2) stearic acid + H_2 → heptadecene + CO + H_2O	3%	+20.2 kJ/mol	Chu et al. (2017)
	c3) stearic acid → heptadecane + CO_2	68%	−23.5 kJ/mol	Chu et al. (2017)
Hydroisomerization/ Hydrocracking	d) n-alkanes → naphtha + jet fuel + diesel	81%	–	Barbera et al. (2020)

The BFD of the advanced scenario was illustrated in Fig. 2, with the main reactions performed in each block reported in Table 2. Differently from the previous case, palm oil is firstly hydrolyzed into glycerol and free fatty acids thanks to the addition of water (e), through the so-called Colgate Emery process, which is the most widely employed technology for oil hydrolysis (Hsu et al., 2021). The employment of this process has a double advantage: on one side, it permits to obtain the free fatty acids without the use of expensive hydrogen; at the same time, it generates glycerol (with approximately 20 wt% concentration), a valuable by-product which will serve to provide hydrogen trough APR (f). Hydrogen is separated from the gaseous mixture thanks to a pressure swing adsorption system (PSA), assuming 95% recovery and 99% purity. The free fatty acids are hence deoxygenated thanks to the hydrogen derived from the APR step (c1-3). Please note that in this case, the HDO reactor does not foresee any propane formation since the triglyceride backbone was already broken during the hydrolysis: therefore, the first step is the saturation of the fatty acids double bonds (g). Afterwards, the HDO reactor effluent undergoes analogous reactions/operations as in the conventional case.

The design of the deoxygenation and hydrocracking/hydroisomerization reactors was based on the analysis performed by Barbera et al. (2020). Specifically, a configuration with multiple intercooled adiabatic trickle bed reactors was chosen to mitigate the exothermic effects of the deoxygenation reactions, while operating under trickle flow regime to maximize conversion and productivity (Ranade et al., 2011).

The reaction conditions are reported in Table 3. Milder operative conditions than conventional vacuum oil cracking were hypothesized since the feedstock is a light oil. In this step, hydrogen was fed in large excess (5 wt% hydrogen/feed ratio): this choice, together with the direct hydrogen quench at the inlet of each stage, allows to mitigate the exothermicity of the reaction. The hydrogen consumption, as well as the yield in jet fuels and by-products (light gas, naphtha, and diesel), was derived from the simulation reported in (Barbera et al., 2020).

Finally, the separation into jet fuel and by-products was carried out in a distillation column.

2.2. Economic analysis

The mass and energy balances previously performed, together with the design information, allowed to evaluate the capital and operating costs of the two scenarios, in order to get an insight on the economic competitiveness of the APR implementation for the SAF production. For this reason, the minimum fuel selling price (MFSP) for the two

Table 3
Reaction conditions in the conventional and advanced scenario (hydrodeoxygenation and hydroisomerization/hydrocracking are assumed to have the same conditions in both scenarios).

Conventional scenario			
Block	Reaction conditions		Reference
Hydrodeoxygenation	Temperature (°C)	400	Chu et al. (2017)
	Pressure (bar)	92	
	H_2/feed ratio (wt.%)	2.7%	
	Catalyst	NiMo/ γ-Al_2O_3	
	Residence time	2 h	
Hydroisomerization/ Hydrocracking	Temperature (°C)	350	Barbera et al. (2020)
	Pressure (bar)	90	
	H_2/feed ratio (wt.%)	3.4%	
	Catalyst	Pt/HZSM-22/γ-Al_2O_3	
	WHSV (h^{-1})	1	
Advanced scenario			
Block	**Reaction conditions**		**Reference**
Hydrolysis	Temperature (°C)	270	Hsu et al. (2021)
	Pressure (bar)	55	
	Oil-to-water weight ratio	2	
	Residence time (h)	2.5	
Aqueous phase reforming	Temperature (°C)	250	Khodabandehloo et al. (2020)
	Pressure (bar)	50	
	Catalyst	$PtCeZrO_2$	
	WHSV (h^{-1})	2.45	

Table 2
List of reactors employed in the advanced scenario. An example of the reactions carried out in each unit is also reported, together with the extent of reaction and enthalpy.

Advanced scenario				Reference
Reactor	Reaction	Extent of reaction	Reaction enthalpy	
Hydrolysis	e) triolein +3 H_2O → 3 oleic acid + glycerol	100%	−321 kJ/mol	(Hsu et al., 2021; Istyami et al., 2018)
Aqueous phase reforming	f) glycerol + 3 H_2O → 7 H_2 + 3 CO_2	93%	+130 kJ/mol	Khodabandehloo et al. (2020)
Hydrodeoxygenation	g) oleic acid + H_2 → stearic acid	100%	−91.7 kJ/mol	Gosselink et al. (2013)
	c1) stearic acid + 3 H_2 → octadecane + 2 H_2O	29%	−129.6 kJ/mol	Chu et al. (2017)
	c2) stearic acid + H_2 → heptadecene + CO + H_2O	3%	+20.2 kJ/mol	Chu et al. (2017)
	c3) stearic acid → heptadecane + CO_2	68%	−23.5 kJ/mol	Chu et al. (2017)
Hydroisomerization/Hydrocracking	d) n-alkanes → naphtha + jet fuel + diesel	81%	–	Barbera et al. (2020)

configurations was estimated. The economic analysis was performed in Microsoft Excel, following the procedure reported in (Turton et al., 2012).

Firstly, total capital investment (TCI) was estimated as the sum of the fixed capital investment (FCI) and working capital (WC). Please note that the cost of land was neglected since it was assumed not relevant for the sake of comparison. FCI includes the costs related to the building of a new plant, therefore it primarily requires the costs associated to the main equipment, such as reactors, heat exchangers, pumps, distillation columns, etc. (the complete lists for both cases are reported in Table S1 and Table S2 of the Supplementary Materials). To do so, the module costing technique was employed (Turton et al., 2012). Thanks to correlations reported therein, this method allows to get the purchased cost of an equipment depending on its type, the working pressure and material of construction (Equation (2) - (Turton et al., 2012)).

$$C_{BM,i} = C^{\circ}_{P,i}\, F_{BM,i} \tag{2}$$

where $C_{BM,i}$ is the bare module cost of the single equipment, $C^{\circ}_{P,i}$ is the purchased cost at base conditions (common material of construction, ambient pressure, etc.) and $F_{BM,i}$ is the bare module cost factor, which takes into consideration all the deviations from base conditions.

The evaluation of the cost estimation is critical in the chemical process industry, and it becomes a challenge in the case of early-stage design, where innovative processes are involved, and limited information are available. Within the classes used by the Association of the Advancement of Cost Estimating International, class 4 was used in this study, which is referred to a preliminary study of feasibility (Cheali et al., 2015).

All costs were inflated to 2019 using the CEPCI factors, while assuming as baseline the corresponding value per each reference ($CEPCI_{1968} = 112$; $CEPCI_{2001} = 397$; $CEPCI_{2014} = 479$; $CEPCI_{2016} = 557$; $CEPCI_{2017} = 568$; $CEPCI_{2019} = 608$) ("Chemical Engineering: The chemical engineering plant cost index," n.d.). Since it was assumed that a new facility is constructed, contingency, fee and auxiliary facilities costs should be added to obtain the FCI. These indicators were evaluated as 15%, 3% and 50% of the total bare module cost, respectively. The summation of these items allows to quantify the fixed capital investment (Equation (3) - (Turton et al., 2012)).

$$FCI = 1.68 \sum_{i=1}^{n} C_{BM,i} \tag{3}$$

The working capital (necessary for inventories of feeds, spare parts, etc.) was assumed as 10% of the FCI. In some cases, the equipment costs were derived from literature values (see Table S1 and Table S2 for the specific reference) and adapted to the chosen plant size by using a suitable scaling factor (i.e., by the so-called six-tenth rule).

The next step in the economic evaluation was the estimation of manufacturing costs (COM), which can be assumed as the summation of direct (DMC) and fixed (FMC) manufacturing costs, in addition to general expenses (GE). DMC consider mainly the cost of raw materials (C_{RM}), waste treatment (C_{WT}), utilities (C_{UT}) and operating labor (C_{OL}); FMC refer to depreciation, taxes and plant overhead; GE are finally related to administration costs, distribution and selling, and R&D. Most of these items are derived from correlations reported in literature, and Equation (4) reports the final correlation excluding depreciation (COM_d) (Turton et al., 2012).

$$COM_d = 0.18\ FCI + 2.73\ C_{OL} + 1.23\ (C_{UT} + C_{WT} + C_{RM}) \tag{4}$$

The price of the main items is shown in Table 4. Please note that green hydrogen utilization was considered as make-up for the scenarios: the impact of different sources of hydrogen was evaluated in the sensitivity analysis.

The profitability of the two scenarios was compared evaluating the necessary MFSP to reach a null net present value (NPV) at the end-of-life plant (Equation (5) - (Turton et al., 2012)), using the discounted cash flow (DCF) method.

$$NPV = \sum_{t=0}^{t=T} \frac{CF_t}{(1+DR)^t} \tag{5}$$

where CF_t is the cash flow at year t, DR is the discount rate and T is the time interval of the investment. The MFSP is to be considered "at the gate", that is, excluding market effects such as contractual agreements with aviation operators etc. (Shila and Johnson, 2021). Please note that the figures evaluated in the twenty-years projection profile do not consider possible variations dependent on inflation trends. The plant was assumed to operate 8000 h per year, for 20 years (Table 5). The construction of the plant was assumed to be performed in 3 years, in which 60% of the FCI was invested at year 1, 30% at year 2 and 10% at year 3. Depreciation was evaluated according to the straight-line method, and the depreciation period was equal to the useful plant lifetime. Salvage value of the equipment at the end of the plant life was assumed to be zero. Income tax rate was considered equal to 30% of the gross profit, while the discount rate was set equal to 10%.

Table 4
Assumptions used for the estimation of manufacturing costs.

Item	Unit	Price	Reference
Raw material			
Palm oil	$/tonne	345	Klein et al. (2018)
Hydrogen	$/kg	6	Zhou and Searle (2022)
Process water	$/tonne	0.48	Zhang et al. (2020)
Utilities			
Electricity	$/kWh	0.087	Barbera et al. (2020)
Natural gas	$/Nm^3	0.13	Barbera et al. (2020)
Cooling tower water	$/kWh	0.35	Barbera et al. (2020)
Medium pressure steam	$/GJ	6.87	Barbera et al. (2020)
High pressure steam	$/GJ	9.83	Barbera et al. (2020)
APR catalyst	$/kg	25	Khodabandehloo et al. (2020)
Wastewater	$/kg$_{COD}$	0.07	Zhu et al. (2013)
Co-Products			
Naphtha	$/L	0.43	Barbera et al. (2020)
Diesel	$/L	0.45	Klein et al. (2018)
Fuel gas	$/MWh	10	Assumption
Others			
Operating labor	$/y	50,000[a]	(Eurostat, n.d.)

[a] Assuming 2000 working hours per employee per year.

2.3. Life-cycle GHG emissions evaluations

The carbon footprint of the SAF production in the conventional and advanced scenarios was assessed following a LCA-approach according to ISO 14040 and ISO 14044 (*BS EN ISO 14040:2006+A1:2020 Environmental management - Life cycle assessment - Principles and framework*, n.d., *BS EN ISO 14044:2006 + A1:2018 + A2:2020 Environmental management - Life cycle assessment - Requirements and guidelines*, n.d.). This methodology foresees (i) the definition of goal and scope, (ii) the inventory analysis, (iii) the impact assessment and (iv) the interpretation of the results. As far as the first step is concerned, the goal was defined as the evaluation of the global warming potential (GWP) of the conventional

Table 5
Assumptions used for the discounted cash flow analysis.

Item	Value
Plant life (y)	20
Construction schedule	Year 1: 60% FCI Year 2: 30% FCI Year 3: 10% FCI
Operating hours (h)	8000
Discount rate	10%
Depreciation	Straight line over the entire operative plant lifetime
Income tax rate	30%
Cost year	2019
Working capital	10% FCI

and advanced biorefinery described above, because this impact category is a key driver in the development of alternative fuels. An attributional assessment with gate-to-gate system boundaries was chosen. CML 2001 baseline (version 2016) method was employed to evaluate the impact on GABI.

The functional unit (FU) was 1 MJ of SAF and the results were reported as grams of CO_2 equivalent per functional unit. The quantification of GHG emissions when different coproducts are present is influenced by the allocation choice. Three criteria are commonly followed, i.e., mass-based, energy-based or value-based allocation. Due to the variability of the biofuel market, only the first two criteria were employed and will be used for the sake of comparison.

Some assumptions were performed, in particular:

- Material and energy for construction were not considered in the LCA in accordance with literature (Seber et al., 2022; Zoppi et al., 2023)
- In GABI database, European mix was used for electricity which includes various sources, such as fossil fuels (41.5%), nuclear (27.6%), wind (8.0%), hydro (12.8%) and others; a similar distribution is reported by the European Commission for 2019 ("Net electricity generation, EU27, 2019," n.d.). Natural gas was used as source of thermal energy
- The cooling thermal power was converted to electricity as described in technical literature (Coulson et al., 2001)
- The electrolyzer used for hydrogen production was modelled based on literature (Sánchez et al., 2020); the performance of the steam reforming (SR) was taken from GABI database. Brown hydrogen data was based on literature (Arcos and Santos, 2023) as well as blue (Oni et al., 2022)
- NiMo catalyst lifetime was set at 1 year, with GHG emission emissions equal to 5.5 kg CO_2 eq./kg_{cat} derived from literature (Snowden-Swan et al., 2016). Pt-based catalyst life time was conservatively set at 1 year (Sladkovskiy et al., 2018), with the data regarding its environmental impact derived from literature, considering 28% of platinum recycling (International Platinum Group Metals Association, 2017)

2.4. Sensitivity and uncertainty analysis

In this study, a sensitivity analysis was carried out to determine the impact of different variables on the minimum selling price of the SAF and on GWP. Plant size (±30%) is correlated with the availability of the feedstock, and it is hence a crucial feature when dealing with biorefineries, whose scalability is often a challenge. Varying the capital cost (±30%) considers the low technology readiness level of the process implemented in these scenarios, particularly for the APR case, and the intrinsic accuracy of the design method followed. SAF yield was modified (±30%) to consider possible improvements (or worsening) in the process efficiency. Palm oil and hydrogen prices were varied as well, with the latter being a key variable since it depends mainly on the production method (e.g., natural gas steam reforming, coal gasification, etc.). Thermal and electric energy prices were modified to take into account pandemic and war impacts on the world energetic scenario. In addition, alternative vegetable oils (soybean, camelina and jatropha) were evaluated due to their different prices and degree of unsaturation, which directly affects the hydrogen consumption. Furthermore, the impact of different hydrogen sources on the GWP was quantified.

Finally, thanks to the use of Monte Carlo simulations, a distribution of NPV was defined (Excel Visual Basic), which can give valuable indications to interested investors while evaluating the risk. A triangular distribution was assigned to the variables with the highest impact derived in the sensitivity analysis After 10,000 iterations, in which the uncertain independent variables were randomly sampled, a cumulative probability distribution of the NPV for the two scenarios was derived.

3. Results and discussion

3.1. Process design

Fig. 3 shows a basic version of the process flow diagram for the conventional scenario (please refer to Table S3 for the stream table).

The SAF yield, estimated as kg of product per kg of fed vegetable oil, was equal to approximately 40%, while it was ca. 25% the yield of naphtha, in line with other data reported in literature (Shahriar and Khanal, 2022). The hydrogen consumption was equal to 0.08 kg_{H2}/kg_{SAF} and it was consumed in the HDO and hydrocracking/hydroisomerization (HI/HC) step by 65.4% and 30.6%, respectively. Please note that the remaining 4% was considered lost during the gas separation step. The hydrogen consumption is higher than typical values found in literature, since some works do not consider hydrogen utilization in the HI/HC reactor, or assume its complete recovery during the separation (Tao et al., 2017). The heat exchanger network was optimized to minimize the external energy requirement. The energy balance showed that 245 $kWh_{th}/tonne_{SAF}$ were consumed, mostly due to the thermal duty in the reboiler (83%), with the remaining accounted by the furnace. The electric energy consumption was equal to 256 kWh_{el}/tonne of SAF, where 70% was attributed to the compressor C1, responsible for the first compression of the make-up hydrogen. The overall energetic efficiency of the plant, measured as the ratio between the energetic output (LHV of naphtha (44.9 MJ/kg), SAF and diesel (43 MJ/kg), fuel gas (20 MJ/kg) (Barbera et al., 2020)) and input (LHV of raw materials and energetic duties) is 75%, in agreement with typical ranges (Shahriar and Khanal, 2022).

Fig. 4 depicts the process flow diagram related to the advanced scenario (Table S4 in the Supplementary material contains the corresponding stream table).

The SAF yield is almost the same as the previous case (38.2%), as well as the naphtha yield (24.2%). The total hydrogen requirement was the same, but the external consumption, i.e., the amount of hydrogen not provided in-situ, decreased by 63% (0.03 kg_{H2}/kg_{SAF}) thanks to the contribution of the APR step. Due to the heating demand of the APR section, there was a 37% rise in consumption compared to the standard case, reaching 336 $kWh_{th}/tonne_{SAF}$. The electric energy consumption was equal to 147 kWh_{el}/tonne of SAF, i.e., −43% with respect to the conventional case. This was due to the lower energetic requirement of the compressor C1 and points out an additional advantage of APR, that is, producing pressurized hydrogen thanks to the pressurization of the liquid feed, which is strongly less expensive than the gas pressurization. The overall energetic efficiency of the plant was equal to 81%, slightly higher than the base case, thanks to the lower global energy request and despite the lower energetic value of the fuel gas (12 MJ/kg) due to the lack of propane.

Table 6 summarizes some key indicators for the two evaluated scenarios.

3.2. Economic assessment results

In the conventional scenario the cost of equipment was about 90 M$. Despite the large variabilities due to the different plant size, a comparison with the values reported by the literature by proper scaling shows that this value is in accordance with previous works (Pavlenko et al., 2019; Shahriar and Khanal, 2022). Fig. 5 (left) shows the distribution of the equipment installation cost. The catalytic reactors play a determinant role in the cost, being approximately 33% the HDO and 56% the HI/HC. This is attributed to their high volume (dealing with a large excess of gaseous hydrogen) and harsh operating conditions (high pressure) which required the use of stainless steel with suitable characteristics (Barbera et al., 2020).

The gas compressors accounted for a 5% of the equipment costs, while the impact of liquid pressurization was negligible, as expected (0.2%). The separation section, which is constituted by high- and low-

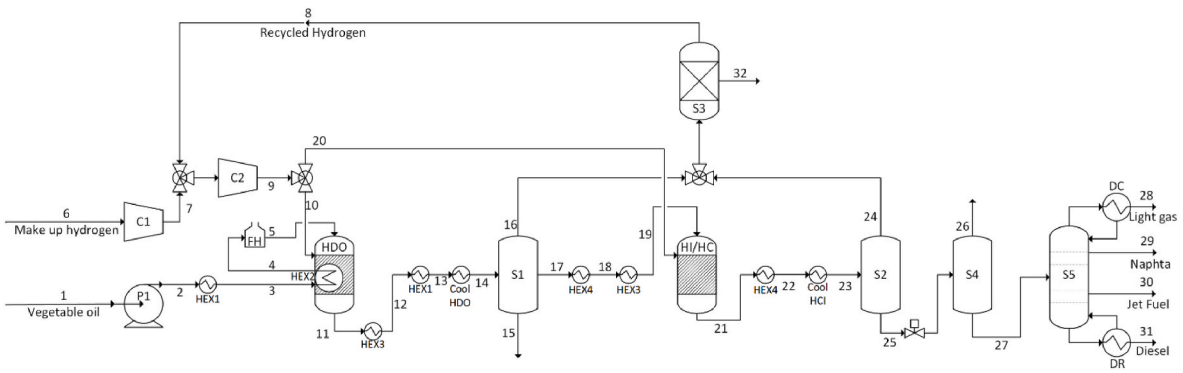

Fig. 3. Simplified process flow diagram of the conventional scenario. The reader is invited to refer to the supplementary information (Table S3) for the mass flow, composition, temperature and pressure of the streams, and to Table S1 for information on the price of the equipment.

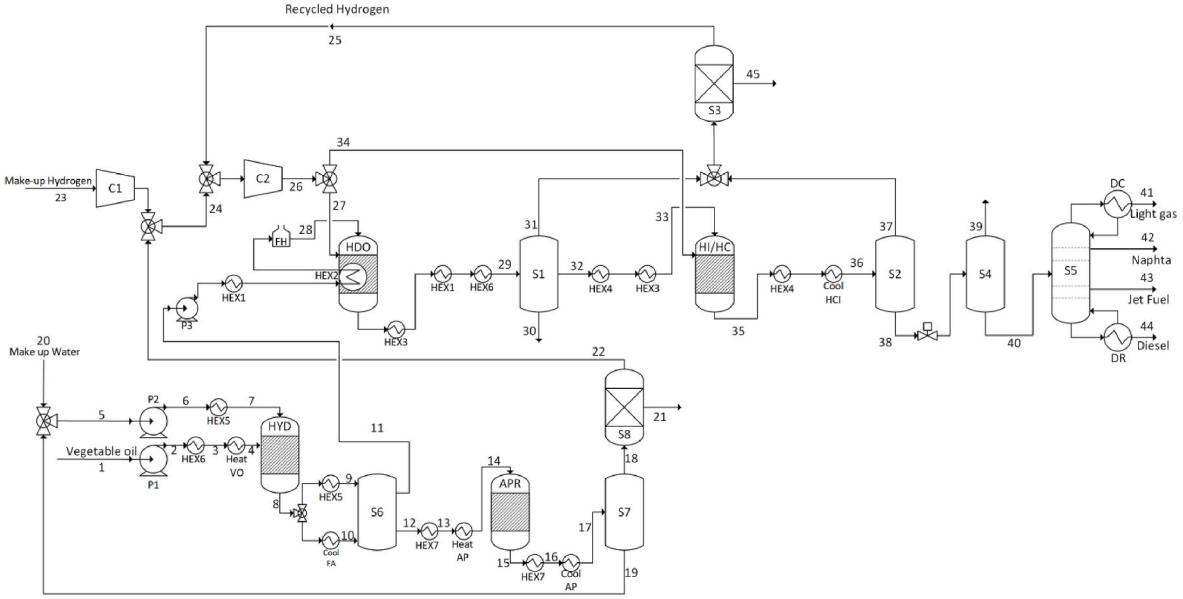

Fig. 4. Simplified process flow diagram of the advanced scenario. The reader is invited to refer to the supplementary information (Table S4) for the mass flow, composition, temperature and pressure of the streams, and to Table S2 for information on the price of the equipment.

Table 6
Main results derived from mass and energy balances in the conventional and advanced scenarios.

	Conventional scenario	Advanced scenario
SAF yield (kg_{SAF}/kg_{OIL})	0.40	0.38
External hydrogen consumption (kg_{H2}/kg_{SAF})	0.08	0.03
Thermal energy requirement ($kWh_{th}/tonne_{SAF}$)	245	336
Electrical energy requirement ($kWh_{el}/tonne_{SAF}$)	256	147
Energetic efficiency (MJ_{out}/MJ_{in})	0.75	0.81

pressure separators, PSA for hydrogen recovery and products distillation column accounted for 2.8%, with PSA showing the highest contribute (50% of the separation section cost). Finally, the heat/cool section, constituted by the heat exchanger network and the reboiler/condenser of the distillation column, ended up in 3%, with the furnace playing the prominent role (45% of the heat/cool section cost). Overall, including the contingency, fees and auxiliary costs, the FCI was equal to 151 M$.

The advanced scenario showed a slight increase of the equipment costs at 95 M$, and Fig. 5 (right) depicts the distribution of the equipment installation cost. The rise was mainly attributed to the APR reactor (ca. 3.5 M$) and to the separation section (ca. 5 M$, vs 3 M$ in the conventional scenario). The compression costs globally decreased with respect to the base case (3.2 M$ vs 4.6 M$), despite the increasing units. This was mainly due to the smaller size of the compressor responsible for the make-up hydrogen pressurization. The higher complexity of the heat exchanger network led to an increase of the section costs by 21%, but due to the low impact of this block on the overall costs, its influence was negligible. By including the contingency, fees and auxiliary costs, the FCI was equal to 160 M$.

Looking at the distribution of the direct manufacturing costs (Fig. 6), 97.3% was attributed to the raw materials (63% to palm oil and 34.2% to hydrogen) in the conventional case. This outcome is commonly found in the literature since the price of the feedstock plays a determinant role in the production costs of SAFs (see the sensitivity analysis in paragraph 3.4 for further evaluations) (Shahriar and Khanal, 2022). Among the remaining items, the compression costs associated with the make-up hydrogen pressurization accounted for 40%, followed by operating labour (26%), costs of the final compression C2 (15%) and reboiler (13%). Overall, the total manufacturing costs (excluding depreciation) were equal to 147.5 M$/y.

Moving to the advanced scenario, the direct manufacturing costs decreased substantially from 98.6 M$/y to 76.9 M$/y (−22%). This is

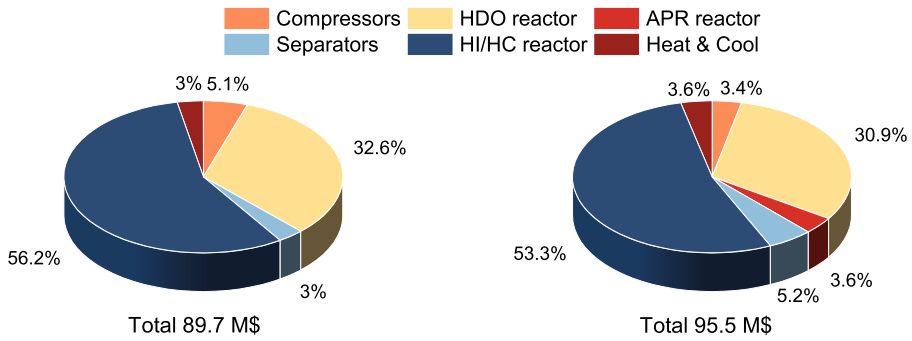

Fig. 5. Equipment breakdown costs for the conventional (left) and advanced (right) scenarios. In addition, the total cost of equipment is reported below. Please note that "Heat & Cool" refers to the cost of the heat exchanger network, as well as the other units necessary for external duties (e.g., furnace, reboiler and condenser).

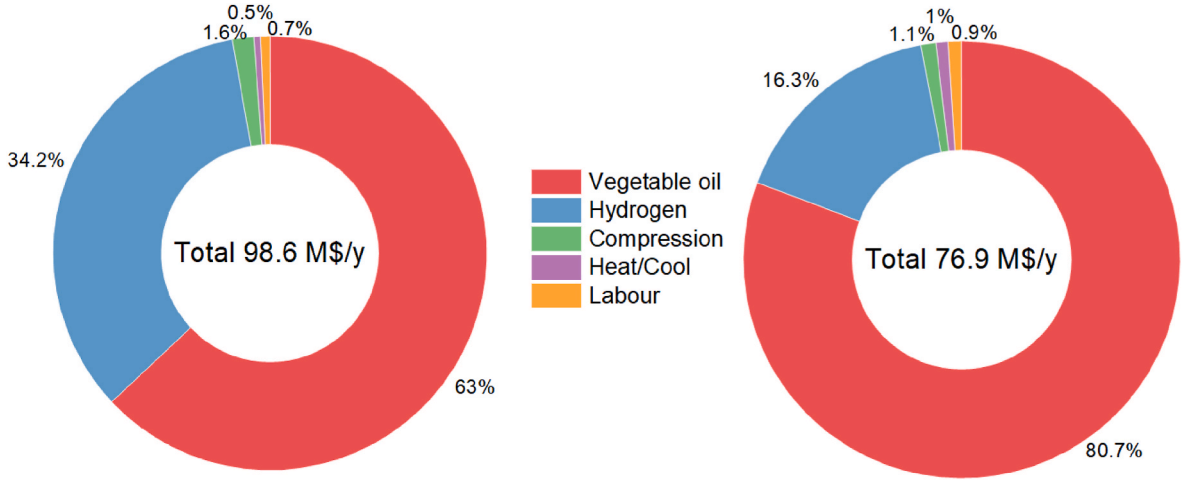

Fig. 6. Direct manufacturing yearly breakdown costs for the conventional (left) and advanced (right) scenarios. In addition, the total cost is reported. Please note that "Heat & Cool" refers to the cost of the external utilities (furnace, medium and high-pressure steam, cooling water).

mainly due to the strong decrease of the hydrogen cost, which thanks to the contribution of the APR section, was reduced from 33.7 M$/y to 12.5 M$/y (−63%). Consequently, the palm oil cost increased its share up to 80.8% of the DMC. The utilities costs decreased from 2 M$/y to 1.5 M$/y, thanks to the lower electric energy demand of compressor C1. The operating labour slightly increased from 0.7 M$/y to 0.75 M$/y due to the higher amount of installed equipment. Overall, the COM_d were equal to 122.6 M$/y, i.e., ca. −17% with respect to the conventional scenario.

The quantification of the FCI and COM_d allowed to perform the discounted cash flow analysis to determine the MFSP in both scenarios. The deterministic economic analysis showed that the advanced scenario performed better than the conventional one thanks to the lower minimum fuel selling price. In fact, it was found out that the MFSP in the conventional scenario was equal to 2.20 $/kg, while it decreased by 17% in the advanced scenario, reaching 1.84 $/kg. These prices, despite being within the values reported in literature (Klein et al., 2018; Shahriar and Khanal, 2022), are significantly higher than the current fossil-based market. Nevertheless, it points out the effectiveness of APR implementation to decrease the SAF cost while providing an alternative and renewable hydrogen source. An attempt for vegetable oil deoxygenation by renewable hydrogen was made by Zech et al. through water electrolysis, but leading to an increase of the production cost by 34% (Zech et al., 2018). Shila et al. reported the difference between having an on-site hydrogen production in contrast to buying hydrogen externally (Shila and Johnson, 2021). The authors pointed out that investing in an on-site hydrogen plant increased the capital cost up to 0.18$/L. Finally, Vivadinar et al. compared different sources of renewable hydrogen (biomass gasification, geothermal electrolysis and solar photovoltaic electrolysis) with SMR, observing that the latter was the technology with the lowest production cost (Vivadinar and Purwanto, 2021).

Please note that the MFSP strongly depends on many variables (e.g., plant size and raw materials prices) which affect its final value: the evaluation of such impact will be discussed in paragraph 3.4.

3.3. Environmental assessment results

Table 7 depicts the inventory list (1 MJ SAF) for the conventional and advanced scenario, pointing out the inputs, outputs and emissions, as well as the dataset used for the assessment.

The assessment showed that the GWP related to the conventional biorefinery is equal to 54.3 g CO_2 eq., while it is 23 g CO_2 eq. in the advanced configuration. It is important to point out that these values are related to a plant which leads to 1 MJ SAF production, but also to naphtha, fuel gas and diesel. Therefore, this value should not be attributed entirely to the production of jet fuel: to do so, allocation should be carried out, and it will be reported later in this paragraph.

Table 7 does not refer to CO_2 emissions. This is because the CO_2 produced in the process (e.g., during decarboxylation of vegetable oil, or during APR) ends up in the fuel gas, so it was not considered as an actual emission source.

Fig. 7 shows the breakdown of the impact among the main items: hydrogen requirement, utilities (electricity, heating and cooling), and catalysts. Hydrogen was the main responsible for the GWP of the plant,

Table 7
Life cycle inventory of 1 MJ SAF production for conventional and advanced scenarios. The dataset used (either in GaBi or from the literature) is added. n.a. not applicable.

Inputs/Outputs/Emissions	Item	Conventional	Advanced	Unit	Dataset
Inputs	Feedstock	22.50	22.50	tonne/h	–
	Process water	0	2.31	tonne/h	Process water (EU-28)
	Hydrogen	0.70	0.26	tonne/h	Green hydrogen modelled according to (Sánchez et al., 2020) Hydrogen steam reforming (DE) for SR Brown hydrogen modelled according to (Arcos and Santos, 2023) Blue hydrogen modelled according to (Oni et al., 2022)
	Electricity	2205.37	1263.36	kWh	Electricity grid mix (EU-28
	Heating	2107.46	2881.74	kWh	Thermal energy from natural gas (EU-28)
	Cooling	307.22	146.64	kWh_{el}	Modelled according to (Coulson et al., 2001)
	Pt (APR cat.)	n.a.	2.49	tonne/h	Modelled according to (International Platinum Group Metals Association, 2017)
	NiMo (HDO cat.)	73.35	70.15	kg/h	Modelled according to (Snowden-Swan et al., 2016)
Output	SAF	8.59	8.59	tonne/h	
	Naphtha	5.45	5.45	tonne/h	
	Fuel gas	7.81	9.9	tonne/h	
	Diesel	0.0576	0.0576	tonne/h	
Emissions	Wastewater	0.85	0.85	tonne/h	Wastewater treatment (EU-28)

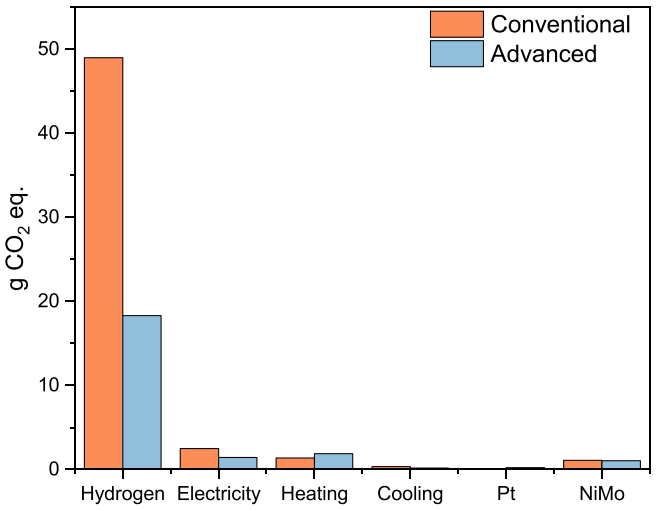

Fig. 7. Breakdown of GWP impact for 1 MJ SAF plant in the conventional and advanced scenarios. The hydrogen bar is referred to the environmental footprint related to its production.

accounting for 90% and 80% of the total impact in the conventional and advanced plant, respectively. This outcome is in accordance with previous works which demonstrated the high carbon footprint related with the use of hydrogen with reference to the SAF production step (Seber et al., 2022; Ukaew et al., 2016). Furthermore, it highlights the importance of the present assessment and the strategic interest towards the implementation of alternative H_2 production routes for SAF development.

As reported above, allocation is necessary when multiple products are obtained. In the present assessment, naphtha, fuel gas and diesel are co-products with SAF. A mass-based and energy-based allocation was followed, and the results are reported in Table 8. As a result, it turns out that the GWP related to the aviation fuel, in the advanced biorefinery is equal to 8.2 g CO_2 eq./MJ following a mass-based allocation (−61% with respect to the conventional one), and 11.7 g CO_2 eq./MJ following an energy-based allocation (−54%). The difference is mostly related to the difference between mass and energy distribution among the products, and particularly because of the fuel gas. Its flow rate is similar to the one of SAF (for both scenarios), but its energetic content is significantly lower, because of the high presence of carbon dioxide in this stream.

In this work, the goal of the LCA is evaluating the possibility of implementing APR as hydrogen source to reduce the impacts associated

Table 8
Mass-based and energy-based allocation of the global warming potential for the two investigated scenarios.

	Conventional scenario		Advanced scenario	
	Mass-based allocation			
	Mass percentage	GWP (g CO_2 eq.)	Mass percentage	GWP (g CO_2 eq.)
SAF	38.5%	20.9	35.5%	8.2
Naphtha	24.5%	13.3	22.6%	5.2
Fuel gas	36.8%	20.0	41.7%	9.6
Diesel	0.3%	0.1	0.2%	0.1
	Energy-based allocation			
	Energy percentage	GWP (g CO_2 eq.)	Energy percentage	GWP (g CO_2 eq.)
SAF	47.3%	25.7	50.7%	11.7
Naphtha	31.4%	17.0	33.7%	7.8
Fuel gas	21.0%	11.4	15.2%	3.5
Diesel	0.3%	0.2	0.3%	0.1

with SAF production. For this reason, the boundaries were limited to the biorefinery, allowing a rigorous evaluation thanks to the available literature and experimental data. This methodological choice is different with respect to several other LCAs performed, where wider boundaries were employed (e.g., including the biomass growth or the fuel utilization) and for this reason a straightforward comparison cannot be carried out.

However, by extrapolating only the production step, a comparison with literature data can be performed. Jet fuel production from different sources was evaluated by Seber et al. (2022). The impact in terms of GHG emissions for MJ of SAF with energy allocation is estimated to be approximately 15 g CO_2 eq./MJ_{SAF} if the same boundaries of this work were considered. With the same approach, a comparison can be made with Yu and coworkers who evaluated different feedstocks and allocation methods (De Jong et al., 2017). The GWP related to jet fuel production for Camelina was approximately to 22 g CO_2 eq./MJ_{SAF} with energy allocation and 17 g CO_2 eq./MJ_{SAF} with mass allocation (23 g CO_2 eq./MJ_{SAF} starting from Jatropha). In both these works the importance of the hydrogen sources is highlighted.

3.4. Sensitivity results

To take into account the uncertainties related to the value of some variables, the influence of plant size, SAF yield, FCI, palm oil costs and energy price was evaluated changing one of them individually. The reason behind this choice is discussed in the following.

One of the most important points for a biorefinery is determining its size. This choice is firstly related to the availability of the feedstock, and it is often a tradeoff between the possibility of implementing an economy of scale and the complexity of long transportation distance. In accordance with the available studies for SAF production, the investigated range was between 120 ktonne/y and 240 ktonne/y (Shahriar and Khanal, 2022). FCI was varied between ±30% due to the accuracy of the followed design method. Palm oil cost (POC) was changed (±50%) due to its high share in the direct manufacturing costs. Finally, energy price was modified (±200%) to take into consideration the actual uncertainties in the energy market due to the post-pandemic and war situation (Jakob Feveile Adolfsen, Friderike Kuik, 2022).

Fig. 8-A summarizes the importance of such variables to drive the most the MFSP. It can be observed that POC affected the most the MFSP, since the MFSP varied ±25% within the investigated range of the variable. This result is in accordance with previous works (Tao et al., 2017; Wang, 2016), and highlights the importance of using low price fats (such as animal fats and greases). At the same time, a stable market for such feedstocks should be developed, and international policies may contribute to this matter.

The modification of the SAF yield played a strong role, leading to a decrease in the selling price with its increase. The trend is in agreement with previous literature (Eswaran et al., 2021). Anyway, HEFA production pathway is the one which permits the highest process yield, in terms of tonne of total fuel per tonne of feedstock (Shahriar and Khanal, 2022).

Slightly less, but still significant, impact can be attributed to the FCI (±11%) and plant size (±6%), while the energy price had a minimal influence. This outcome is coherent with what was observed in paragraph 3.2, i.e., its low share in the direct manufacturing costs. Therefore, it can be derived that the SAF price can be reduced mainly by actuating policies which decrease the feedstock costs and building big plants; therefore, the development of a resilient supply chain and so-called biohubs can facilitate the expansion of this sector. On the other hand, fluctuations in the energy market can have a negligible effect. A similar trend was observed in the advanced scenario (Fig. 8-B). It is noted that, in this case, the MFSP varied ±30% within the investigated range of POC because of its higher influence in determining the manufacturing costs; moreover, a slightly higher variation was also observed for the FCI (±14%) and plant size (±8%), attributed to the higher capital expenditure of the advanced scenario.

Furthermore, the impact of the type of feedstock and hydrogen was assessed. The former has a relevant influence for two main reasons. Firstly, because of its proper cost, since it was shown that the cost of the raw material is the most important one for the manufacturing costs; secondly, the different triglycerides profile, and particularly the presence of unsaturated bonds, affects the hydrogen consumption. To estimate the first effect, we evaluated the employment of other common vegetable oil sources, such as jatropha, camelina and soybean oil, whose composition is reported in Table 9.

Their impact was quantified considering their different triglyceride distribution and price, and assuming that the intrinsic kinetics of the fatty acid is not significantly influenced (i.e., only the hydrogen uptake changes according to the unsaturation degree of the molecules). The hydrogen need was higher for soybean than camelina and similar for palm and jatropha. The influence of the feedstock nature on the MFSP is reported in Fig. 9-A. The global difference is mainly due to the modification of the feedstock price, which embeds most of the production cost. In fact, the MFSP ranking follows the feedstock cost (jatropha > soybean > palm > camelina), despite the hydrogen consumption ranking is different.

Hydrogen price greatly depends on the technologies employed for its production (Table 9). Fig. 9-B depicts the modification moving from the reference chosen in this work (green hydrogen) to the conventional industrial H_2 production (grey hydrogen, i.e., from natural gas steam reforming), through brown hydrogen (produced from coal gasification) and blue hydrogen (produced from fossil fuels but in tandem with carbon capture and storage). Moving towards high-carbon hydrogen led to a decrease of the MFSP. Due to the higher external H_2 demand, this variation affected more strongly the conventional scenario, where the lowest MFSP using grey hydrogen was equal to 1.75 $/kg (−21% compared to green hydrogen source); on the other hand, for the

Table 9
Sensitivity analysis on vegetable oil and hydrogen source. In the table, their prices are reported, as well as the composition of the vegetable oil.

Vegetable oil				
	Palm oil (Klein et al., 2018)	Jatropha oil (Wang, 2016)	Camelina oil (Monte et al., 2022)	Soybean oil (Ndiaye et al., 2006)
Tripalmitin	15%	14.2%	6.2%	11.3%
Triolein	44%	44.7%	16.1%	23.6%
Trilinolein	32%	32.8%	54.3%	54.7%
Tristearin	9%	7.2%	2.6%	3.5%
Trilinolenin	0%	0.2%	0%	6.9%
Triarachidin	0%	0.2%	18.5%	0%
Trierucin	0%	0%	2.3%	0%
Price ($/tonne)	345	500	260	430
Hydrogen source				
	Green (Zhou and Searle, 2022)	Brown (International Energy Agency (IEA), n.d.)	Blue (Yu et al., 2021)	Grey (Yukesh Kannah et al., 2021)
Price ($/kg)	6	2.5	2	1.5

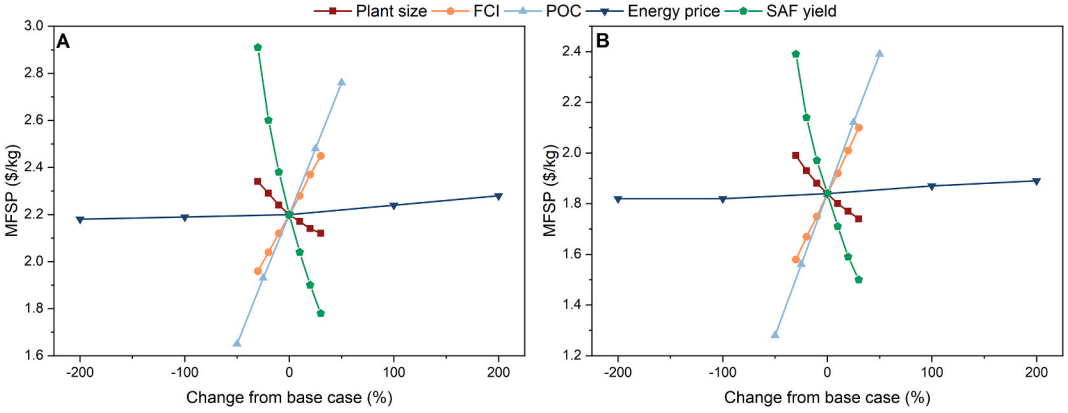

Fig. 8. Sensitivity analysis of MFSP for SAF production in the conventional (A) and advanced (B) scenario.

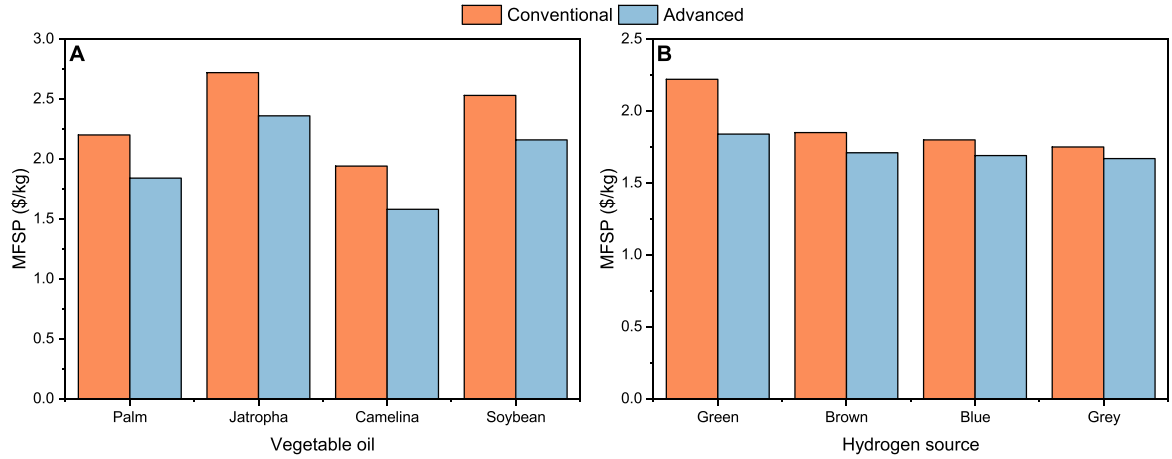

Fig. 9. Influence of vegetable oil (A) and hydrogen source (B) on MFSP for the two investigated scenarios.

advanced scenario, the maximum decrease was ca. −10%, because of the lower influence of the hydrogen price on the plant economics (see Fig. 6-right). It is important to observe that the employment of APR + green hydrogen make up was still competitive under an economic point of view with the use of fossil grey hydrogen in the base case (1.84 vs 1.75 $/kg, respectively, and hence - 5%).

As reported in paragraph 3.3, the source of hydrogen has a prominent role on the definition of SAF environmental footprint. However, this is strongly correlated with the followed production route. In the base case, hydrogen production by electrolysis was assumed (i.e., green hydrogen). The impact of such production route is mainly associated with the electricity consumption, and hence on the grid mix. As stated in paragraph 2.3, the european grid mix (EGM) was used herein. Nevertheless, this composition is not fixed with time; in other words, the implementation of decarbonized sources of electricity will gradually decrease such impact. Fig. 10 shows the results associated with this sensitivity analysis (using energy-based allocation for the sake of comparison). Furthermore, analogously to the economic evaluation performed above, a comparison with other sources of hydrogen was performed.

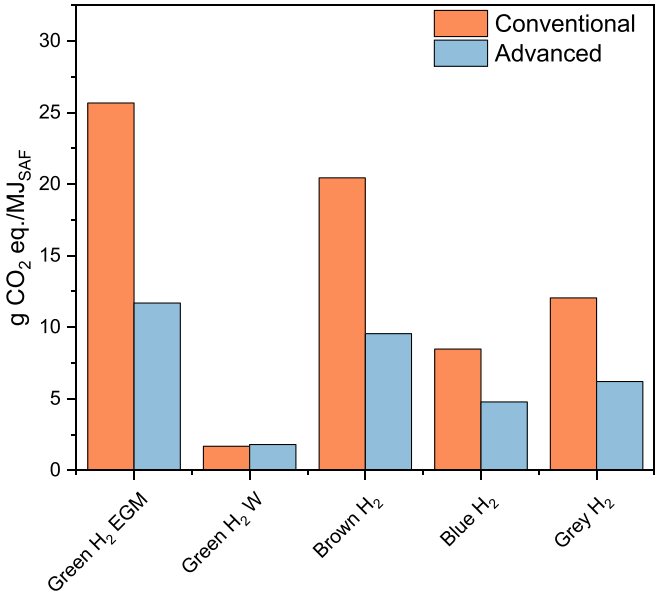

Fig. 10. Influence of hydrogen source on SAF GWP. EGM refers to the electricity derived from European grid mix, while W refers to the one produced with wind power.

Brown hydrogen, is the second most impactful type of hydrogen (Arcos and Santos, 2023), followed by grey and blue hydrogen, where 85% carbon capture was reached (Oni et al., 2022). If wind (W) is used as electric source, the GWP strongly decreased by 93% for the conventional scenario and by 83% for the advanced one, so that the two scenarios were almost equal. This result further highlights how APR can be a competitive strategy even in the case of a fully decarbonized source of electricity.

3.5. Stochastic analysis

In conclusion, a stochastic approach was followed through a Monte Carlo analysis in order to evaluate the investment risk and the uncertainties of the environmental assessment. This tool allows to derive a distribution of the desired economic and environmental output, rather than a determined value.

Due to their highlighted impact on the economic profitability of the plant, a triangular distribution of the plant size, fixed capital investment and vegetable oil price was assumed, within the same range used for the sensitivity analysis. Fig. 11 shows the obtained results for the conventional and advanced scenarios, considering the minimum fuel selling

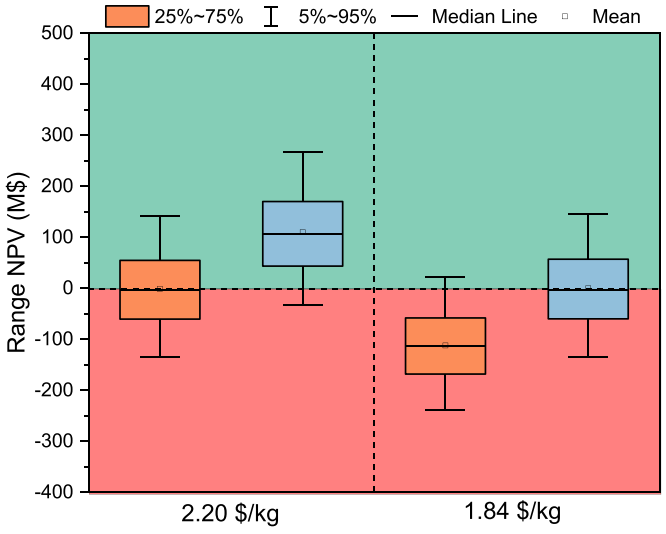

Fig. 11. Box-Whisker plot for the conventional (orange) and advanced (blued) scenarios assuming two selling prices. The green area refers to the iterations ended up in positive NPV, while red area refers to the ones ended up in negative NPV. (For interpretation of the references to colour in this figure legend, the reader is referred to the Web version of this article.)

prices found in paragraph 3.2 as actual selling prices. The green area shows the zero-risk zone, where the net present value is positive; vice versa, the red area indicates the risk zone, where the net present value is negative. The conventional scenario is equally distributed between the two areas when the corresponding minimum selling price found in the deterministic analysis was used, with a span equal to ca. ± 150 M$; on the other hand, if the same price is used in the advanced scenario, only 11% of the 10000 iterations analyzed are in the risk zone. Conversely, if the distribution is the same for the advanced scenario using the corresponding MFSP, the use of such price in the conventional scenario leads to a 91% probability of ending up in the risk zone.

3.6. Remarks and outlook

In conclusion, it is worth pointing out some key features of the novel concept proposed herein, together with open issues.

The modification of process flow diagram with the introduction of the APR step allowed to significantly decrease the external hydrogen demand. The available literature has focused mainly on the deployment of electrolysis-derived hydrogen (Zech et al., 2018). Comparative results with steam reforming-derived hydrogen showed that the latter is still the technically favorable option, with further issues related to H_2 storage created when dynamic scenarios are assumed (Müller-Langer et al., 2019). On the other hand, we showed herein that APR is economically competitive (−5%) with steam reforming as well, with the further advantage that a storage is not required.

The proposal of APR implementation has important consequences also under the environmental point of view. As reported from other studies, hydrogen production is the main responsible for GHG emissions in HEFA process (Pavlenko and Searle, 2021). It was shown here that the most common alternative, green hydrogen, has an even higher environmental footprint than steam reforming when powered by the actual energetic mix (in Europe). On the other hand, the advanced scenario depicted in this work may lead to a decrease with respect to steam reforming (−49%) and to comparable results also in the long term, when only low-carbon electricity may be available (+7%).

One important limitation with regards to APR implementation is due to its technological development level. To the best of our knowledge, there are no commercial examples of plants which aims at hydrogen production, therefore important issues related, but not limited to, catalyst stability, should be assessed. This is indeed vital when noble metals are used.

One final important aspect is related to the perspective of SAF deployment. In 2019, SAF production accounted for only 0.05% of the jet fuel demand, with the HEFA pathway depicted in this work as conventional scenario being the main route because of the proven and well understood technology (O'Malley et al., 2021). In the near-medium term, this pathway is the one with the most promising impact, while other technologies are not expected to provide a key contribution in such limited timeframe because of the lower TRL. The importance of oil-based feedstocks was reported by Su-ungkavatin et al., who recently performed a semi-quantitative assessment of four strategies for the aviation sector, namely biofuels, electrofuels, battery and hydrogen (Su-ungkavatin et al., 2023). They observed that in the near-term future (2030) HEFA stands out with respect to other biofuels, and it is only second to hydrogen technology based on alkaline electrolysis. Furthermore, the International council on clean transportation estimated that, taking into account harvesting capability, ecological value and alternative uses, oil feedstocks can account for ca. 1.9% of total jet fuel demand in 2030 (1.2 Mtonne/y): this is the highest SAF share (35%) with respect to other possible feedstocks evaluated for the aviation sector, such as agricultural and forestry residues, municipal and industrial waste, etc. (O'Malley et al., 2021).

However, the European Union set a gradual but increasing share of SAF up to 70% by 2050, assuming ca. 50 Mtonne per year of total jet fuel demand (Shehab et al., 2023). In this long term, most of the works agrees that the HEFA pathway from vegetable oils could not significantly expand mainly because of the low biomass availability and geographical limitations of the oil crops. Smaller regional-size business models have been proposed for the configuration of the supply chain (Martinez-Valencia et al., 2021), while an alternative feedstock with higher potential productivity is constituted by microalgae, but their high cost and low scale of development currently limit its implementation in most of the assessments (Lim et al., 2021). Apart from electrification and batteries, the technologies that could be implemented are gasification coupled to Fisher-Tropsch, alcohol to jet (ATJ) and sugar to hydrocarbons (SDHC), which are based on biomass as well, but not limited to the availability of oleaginous crops (Okolie et al., 2023). Interestingly, since an hydrogenation step is necessary also in the cited technologies, aqueous phase reforming may find its own spot to provide an alternative hydrogen source even in such routes, as reported in previous works of the authors (Pipitone et al., 2020; Zoppi et al., 2021). Overall, since there is no silver bullet for the decarbonization of the aviation sector, HEFA pathways remains one of the main players, particularly taking into account the possibility of valorizing waste feedstocks and shifting the present portfolio of utilization (like redirecting biodiesel production to SAF) (IEA - International Energy Agency, 2022). One possible limitation with regards to the technology presented herein is that waste oils may contain a higher fraction of free fatty acids and a lower fraction of triglycerides, and hence glycerol, overall decreasing the fraction of hydrogen provided in situ.

4. Conclusions

In this work, a techno-economic and life-cycle GHG assessment was carried out in a biorefinery plant for sustainable aviation fuel production employing in-situ produced hydrogen via aqueous phase reforming. Differently from the conventional design, the feedstock was firstly hydrolyzed to glycerol and free fatty acids, with the former converted into hydrogen via APR. This new process was technically and environmentally assessed as a possible strategy to improve the actual HEFA pathway. It was found that the minimum fuel selling price was equal to 1.84 $/kg, which is 17% lower than the SAF production based on electrolysis-derived hydrogen. Capital investment was found 6.6% higher, while direct manufacturing costs were 22% lower, thanks to the lower external hydrogen demand and compression costs. A broad sensitivity analysis was carried out, showing that the vegetable oil price and SAF yield have the highest impact on the determination of the MFSP, followed by the plant size and the uncertainty on the capital equipment costs. On the other hand, energy prices had a negligible impact thanks to the optimized heat exchanger network. Under the environmental point of view, gate-to-gate CO_2 eq. emissions were found 54% lower than the conventional case when APR was implemented (11.7 g CO_2 eq./MJ_{SAF} with energy-based allocation). More importantly, the sensitivity analysis highlighted that the advanced scenario would be competitive also for the case in which green hydrogen is derived from renewable energy sources.

In conclusion, the insights provided in this work demonstrate that the valorization of glycerol backbone through APR is a technically and environmentally feasible new option for the implementation of SAF production technology.

CRediT authorship contribution statement

Giuseppe Pipitone: Conceptualization, Methodology, Formal analysis, Visualization, Writing – original draft, Writing – review & editing. **Giulia Zoppi:** Conceptualization, Methodology, Formal analysis, Writing – original draft, Writing – review & editing. **Raffaele Pirone:** Supervision, Project administration. **Samir Bensaid:** Conceptualization, Supervision, Project administration.

Declaration of competing interest

The authors declare that they have no known competing financial interests or personal relationships that could have appeared to influence the work reported in this paper.

Data availability

Data used in this work were referenced and are available in literature

Appendix A. Supplementary data

Supplementary data to this article can be found online at https://doi.org/10.1016/j.jclepro.2023.138141.

References

Adolfsen, Jakob Feveile, Friderike Kuik, E.M.L., T, S., 2022. The impact of the war in Ukraine on euro area energy markets [WWW Document]. URL. https://www.ecb.europa.eu/pub/economic-bulletin/focus/2022/html/ecb.ebbox202204_01~68ef3c3dc6.en.html.

Arcos, J.M.M., Santos, D.M.F., 2023. The hydrogen color spectrum: techno-economic analysis of the available technologies for hydrogen production. Gases 3, 25–46. https://doi.org/10.3390/gases3010002.

Barbera, E., Naurzaliyev, R., Asiedu, A., Bertucco, A., Resurreccion, E.P., Kumar, S., 2020. Techno-economic analysis and life-cycle assessment of jet fuels production from waste cooking oil via in situ catalytic transfer hydrogenation. Renew. Energy 160, 428–449. https://doi.org/10.1016/j.renene.2020.06.077.

Bashir, M.A., Lima, S., Jahangiri, H., Majewski, A.J., Hofmann, M., Hornung, A., Ouadi, M., 2022. A step change towards sustainable aviation fuel from sewage sludge. J. Anal. Appl. Pyrolysis 163, 105498. https://doi.org/10.1016/j.jaap.2022.105498.

Bhutto, A.W., Qureshi, K., Abro, R., Harijan, K., Zhao, Z., Bazmi, A.A., Abbas, T., Yu, G., 2016. Progress in the production of biomass-to-liquid biofuels to decarbonize the transport sector-prospects and challenges. RSC Adv. 6, 32140–32170. https://doi.org/10.1039/c5ra26459f.

BS EN ISO 14040:2006+A1:2020 Environmental Management - Life Cycle Assessment - Principles and Framework, (n.d).

BS EN ISO 14044:2006 + A1:2018 + A2:2020 Environmental Management - Life Cycle Assessment - Requirements and Guidelines, (n.d).

Cheali, P., Gernaey, K.V., Sin, G., 2015. Uncertainties in early-stage capital cost estimation of process design - a case study on biorefinery design. Front. Energy Res. 3, 1–13. https://doi.org/10.3389/fenrg.2015.00003.

Chemical Engineering. The chemical engineering plant cost index [WWW Document], n.d. URL. https://www.chemengonline.com/pci-home. accessed 2.13.23.

Chu, P.L., Vanderghem, C., MacLean, H.L., Saville, B.A., 2017. Process modeling of hydrodeoxygenation to produce renewable jet fuel and other hydrocarbon fuels. Fuel 196, 298–305. https://doi.org/10.1016/j.fuel.2017.01.097.

Cortright, R.D., Davda, R.R., Dumesic, J.A., 2002. Hydrogen from catalytic reforming of biomass-derived hydrocarbons in liquid water. Nature 418, 964–967. https://doi.org/10.1038/nature01009.

Costa, C.Z., Sousa-Aguiar, E.F., Couto, M.A.P.G., Filho, J.F.S. de C., 2020. Hydrothermal treatment of vegetable oils and fats aiming at yielding hydrocarbons: a review. Catalysts 10. https://doi.org/10.3390/catal10080843.

Coulson, J.M., Richardson, K.F., Backhurst, J.R., Harker, J.H., 2001. Coulson & Richardson's Chemical Engineering, sixth ed. (Chemical Engineering).

Crisostomo, C.A.B., Almeida, T.S.S., Soares, R.R., 2021. Towards Triglycerides-Based Biorefineries : Hydrolysis-Reforming-Hydrogenation in One-Pot over Ni/γ -Al 2 O 3 Based Catalysts, vol. 367, pp. 124–136.

De Jong, S., Antonissen, K., Hoefnagels, R., Lonza, L., Wang, M., Faaij, A., Junginger, M., 2017. Life-cycle analysis of greenhouse gas emissions from renewable jet fuel production. Biotechnol. Biofuels 10, 1–18. https://doi.org/10.1186/s13068-017-0739-7.

Domínguez-Barroso, M.V., Herrera, C., Larrubia, M.A., Alemany, L.J., 2016. Diesel oil-like hydrocarbon production from vegetable oil in a single process over Pt-Ni/Al2O3 and Pd/C combined catalysts. Fuel Process. Technol. 148, 110–116. https://doi.org/10.1016/j.fuproc.2016.02.032.

Domínguez-Barroso, V., Herrera, C., Larrubia, M.Á., Alemany, L.J., 2019. Coupling of glycerol-APR and in situ hydrodeoxygenation of fatty acid to produce hydrocarbons. Fuel Process. Technol. 190, 21–28. https://doi.org/10.1016/j.fuproc.2019.03.011.

Eswaran, S., Subramaniam, S., Geleynse, S., Brandt, K., Wolcott, M., Zhang, X., 2021. Techno-economic analysis of catalytic hydrothermolysis pathway for jet fuel production. Renew. Sustain. Energy Rev. 151, 111516 https://doi.org/10.1016/j.rser.2021.111516.

Eurostat, n.d.. Wages and labour costs [WWW Document]. URL. https://ec.europa.eu/eurostat/statistics-explained/index.php?title=Wages_and_labour_costs#Labour_costs.

Fasolini, A., Cucciniello, R., Paone, E., Mauriello, F., Tabanelli, T., 2019. A short overview on the hydrogen production via aqueous phase reforming (APR) of cellulose, C6-C5 sugars and polyols. Catalysts 9. https://doi.org/10.3390/catal9110917.

Gosselink, R.W., Hollak, S.A.W., Chang, S.W., Van Haveren, J., De Jong, K.P., Bitter, J.H., Van Es, D.S., 2013. Reaction pathways for the deoxygenation of vegetable oils and related model compounds. ChemSusChem 6, 1576–1594. https://doi.org/10.1002/cssc.201300370.

Han, J., Elgowainy, A., Cai, H., Wang, M.Q., 2013. Life-cycle analysis of bio-based aviation fuels. Bioresour. Technol. 150, 447–456. https://doi.org/10.1016/j.biortech.2013.07.153.

Heyne, J., Rauch, B., Le Clercq, P., Colket, M., 2021. Sustainable aviation fuel prescreening tools and procedures. Fuel 290, 120004. https://doi.org/10.1016/j.fuel.2020.120004.

Hossain, M.Z., Chowdhury, M.B.I., Jhawar, A.K., Xu, W.Z., Charpentier, P.A., 2018. Continuous low pressure decarboxylation of fatty acids to fuel-range hydrocarbons with in situ hydrogen production. Fuel 212, 470–478. https://doi.org/10.1016/j.fuel.2017.09.092.

Hsu, H.W., Chang, Y.H., Wang, W.C., 2021. Techno-economic analysis of used cooking oil to jet fuel production under uncertainty through three-, two-, and one-step conversion processes. J. Clean. Prod. 289, 125778 https://doi.org/10.1016/j.jclepro.2020.125778.

Hwang, K.R., Choi, I.H., Choi, H.Y., Han, J.S., Lee, K.H., Lee, J.S., 2016. Bio fuel production from crude Jatropha oil; Addition effect of formic acid as an in-situ hydrogen source. Fuel 174, 107–113. https://doi.org/10.1016/j.fuel.2016.01.080.

IEA - International, 2022. Energy agency. In: Renewables 2022. IEA, Paris. Analysis forecast to 2027 158.

International Energy Agency (IEA), n.d, 2019. Global Average Levelised Cost of Hydrogen Production by Energy Source and Technology and 2050 [WWW Document]. URL. https://www.iea.org/data-and-statistics/charts/global-average-levelised-cost-of-hydrogen-production-by-energy-source-and-technology-2019-and-2050.

International Platinum Group Metals Association, 2017. The Life Cycle Assessment of Platinum Group Metals.

Issariyakul, T., Dalai, A.K., 2014. Biodiesel from vegetable oils. Renew. Sustain. Energy Rev. 31, 446–471. https://doi.org/10.1016/j.rser.2013.11.001.

Istyami, A.N., Soerawidjaja, T.H., Prakoso, T., 2018. Mass balances and thermodynamics study of thermal triglyceride hydrolysis. MATEC Web Conf. 156, 1–5. https://doi.org/10.1051/matecconf/201815605013.

Jęczmionek, Ł., Porzycka-Semczuk, K., 2014. Hydrodeoxygenation, decarboxylation and decarbonylation reactions while co-processing vegetable oils over a NiMo hydrotreatment catalyst. Part I: thermal effects - theoretical considerations. Fuel 131, 1–5. https://doi.org/10.1016/j.fuel.2014.04.055.

Khodabandehloo, M., Larimi, A., Khorasheh, F., 2020. Comparative process modeling and techno-economic evaluation of renewable hydrogen production by glycerol reforming in aqueous and gaseous phases. Energy Convers. Manag. 225, 113483 https://doi.org/10.1016/j.enconman.2020.113483.

Klein, B.C., Chagas, M.F., Junqueira, T.L., Rezende, M.C.A.F., Cardoso, T. de F., Cavalett, O., Bonomi, A., 2018. Techno-economic and environmental assessment of renewable jet fuel production in integrated Brazilian sugarcane biorefineries. Appl. Energy 209, 290–305. https://doi.org/10.1016/j.apenergy.2017.10.079.

Kouzu, M., Kojima, M., Mori, K., Yamanaka, S., 2021. Catalytic deoxygenation of triglyceride into drop-in fuel under hydrothermal condition with the help of in-situ hydrogen production by APR of glycerol by-produced. Fuel Process. Technol. 217, 106831 https://doi.org/10.1016/j.fuproc.2021.106831.

Kubičková, I., Snåre, M., Eränen, K., Mäki-Arvela, P., Murzin, D.Y., 2005. Hydrocarbons for diesel fuel via decarboxylation of vegetable oils. Catal. Today 106, 197–200. https://doi.org/10.1016/j.cattod.2005.07.188.

Lim, J.H.K., Gan, Y.Y., Ong, H.C., Lau, B.F., Chen, W.H., Chong, C.T., Ling, T.C., Klemeš, J.J., 2021. Utilization of microalgae for bio-jet fuel production in the aviation sector: challenges and perspective. Renew. Sustain. Energy Rev. 149 https://doi.org/10.1016/j.rser.2021.111396.

Martinez-Hernandez, E., Ramírez-Verduzco, L.F., Amezcua-Allieri, M.A., Aburto, J., 2019. Process simulation and techno-economic analysis of bio-jet fuel and green diesel production — minimum selling prices. Chem. Eng. Res. Des. 146, 60–70. https://doi.org/10.1016/j.cherd.2019.03.042.

Martinez-Valencia, L., Garcia-Perez, M., Wolcott, M.P., 2021. Supply chain configuration of sustainable aviation fuel: review, challenges, and pathways for including environmental and social benefits. Renew. Sustain. Energy Rev. 152, 111680 https://doi.org/10.1016/j.rser.2021.111680.

Monte, D.M. del, Cruz, P.L., Dufour, J., 2022. SAF production from cameline oil hydrotreatment: a technoeconomic assessment of alternative process configurations. Fuel 324, 124602. https://doi.org/10.1016/j.fuel.2022.124602.

Müller-Langer, F., Oehmichen, K., Dietrich, S., Zech, K.M., Reichmuth, M., Weindorf, W., 2019. PTG-HEFA hybrid refinery as example of a SynBioPTx concept-results of a feasibility analysis. Appl. Sci. 9 https://doi.org/10.3390/app9194047.

Ndiaye, P.M., Franceschi, E., Oliveira, D., Dariva, C., Tavares, F.W., Oliveira, J.V., 2006. Phase behavior of soybean oil, castor oil and their fatty acid ethyl esters in carbon dioxide at high pressures. J. Supercrit. Fluids 37, 29–37. https://doi.org/10.1016/j.supflu.2005.08.002.

Net electricity generation, EU27, 2019 [WWW Document], n.d. URL. https://ec.europa.eu/eurostat/statistics-explained/index.php?title=File:Net_electricity_generation,_EU27,_2019_(%25_based_on_GWh).png. (Accessed 5 January 2022).

Ng, K.S., Farooq, D., Yang, A., 2021. Global biorenewable development strategies for sustainable aviation fuel production. Renew. Sustain. Energy Rev. 150, 111502 https://doi.org/10.1016/j.rser.2021.111502.

Okolie, J.A., Awotoye, D., Tabat, M.E., Okoye, P.U., Epelle, E.I., Ogbaga, C.C., Güleç, F., Oboirien, B., 2023. Multi-criteria decision analysis for the evaluation and screening of sustainable aviation fuel production pathways. iScience 26, 106944. https://doi.org/10.1016/j.isci.2023.106944.

Oni, A.O., Anaya, K., Giwa, T., Di Lullo, G., Kumar, A., 2022. Comparative assessment of blue hydrogen from steam methane reforming, autothermal reforming, and natural gas decomposition technologies for natural gas-producing regions. Energy Convers. Manag. 254, 115245 https://doi.org/10.1016/j.enconman.2022.115245.

O'Malley, J., Pavlenko, N., Searle, S., 2021. Estimating sustainable aviation fuel feedstock availability to meet growing European Union demand - international Council on Clean Transportation. Int. Counc. Clean Transp.

Pavlenko, N., Searle, S., 2021. Assessing the sustainability implications of alternative aviation fuels. Int. Counc. Clean Transp.

Pavlenko, N., Searle, S., Christensen, A., 2019. The Cost of Supporting Alternative Jet Fuels in the European Union. ICCT Working Paper 2019-05.

Pipitone, G., Zoppi, G., Frattini, A., Bocchini, S., Pirone, R., Bensaid, S., 2020. Aqueous phase reforming of sugar-based biorefinery streams: from the simplicity of model compounds to the complexity of real feeds. Catal. Today 345, 267–279. https://doi.org/10.1016/j.cattod.2019.09.031.

Ranade, V.V., Chaudhari, R.V., Gunjal, P.R., 2011. Trickle Bed Reactors; Reactor Engineering & Applications. https://doi.org/10.1016/b978-0-444-52738-7.10001-4.

Sadhukhan, J., Sen, S., 2021. A novel mathematical modelling platform for evaluation of a novel biorefinery design with Green hydrogen recovery to produce renewable aviation fuel. Chem. Eng. Res. Des. 175, 358–379. https://doi.org/10.1016/j.cherd.2021.09.014.

Salkuti, S.R., 2022. Emerging and advanced green energy technologies for sustainable and resilient future grid. Energies 15. https://doi.org/10.3390/en15186667.

Sánchez, M., Amores, E., Abad, D., Rodríguez, L., Clemente-Jul, C., 2020. Aspen Plus model of an alkaline electrolysis system for hydrogen production. Int. J. Hydrogen Energy 45, 3916–3929. https://doi.org/10.1016/j.ijhydene.2019.12.027.

Scaldaferri, C.A., Pasa, V.M.D., 2019. Hydrogen-free process to convert lipids into bio-jet fuel and green diesel over niobium phosphate catalyst in one-step. Chem. Eng. J. 370, 98–109. https://doi.org/10.1016/j.cej.2019.03.063.

Seber, G., Escobar, N., Valin, H., Malina, R., 2022. Uncertainty in life cycle greenhouse gas emissions of sustainable aviation fuels from vegetable oils. Renew. Sustain. Energy Rev. 170 https://doi.org/10.1016/j.rser.2022.112945.

Shahriar, M.F., Khanal, A., 2022. The current techno-economic, environmental, policy status and perspectives of sustainable aviation fuel (SAF). Fuel 325, 124905. https://doi.org/10.1016/j.fuel.2022.124905.

Shehab, M., Moshammer, K., Franke, M., Zondervan, E., 2023. Analysis of the potential of meeting the EU's sustainable aviation fuel targets in 2030. Sustainability 15, 9266. https://doi.org/10.3390/su15129266, 2050.

Shila, J., Johnson, M.E., 2021. Techno-economic analysis of Camelina-derived hydroprocessed renewable jet fuel within the US context. Appl. Energy 287, 116525. https://doi.org/10.1016/j.apenergy.2021.116525.

Sladkovskiy, D.A., Godina, L.I., Semikin, K.V., Sladkovskaya, E.V., Smirnova, D.A., Murzin, D.Y., 2018. Process design and techno-economical analysis of hydrogen production by aqueous phase reforming of sorbitol. Chem. Eng. Res. Des. 134, 104–116. https://doi.org/10.1016/j.cherd.2018.03.041.

Snowden-Swan, L.J., Spies, K.A., Lee, G.J., Zhu, Y., 2016. Life cycle greenhouse gas emissions analysis of catalysts for hydrotreating of fast pyrolysis bio-oil. Biomass Bioenergy 86, 136–145. https://doi.org/10.1016/j.biombioe.2016.01.019.

Su-ungkavatin, P., Tiruta-Barna, L., Hamelin, L., 2023. Biofuels, electrofuels, electric or hydrogen?: a review of current and emerging sustainable aviation systems. Prog. Energy Combust. Sci. 96, 101073 https://doi.org/10.1016/j.pecs.2023.101073.

Tao, L., Milbrandt, A., Zhang, Y., Wang, W.C., 2017. Techno-economic and resource analysis of hydroprocessed renewable jet fuel. Biotechnol. Biofuels 10, 1–16. https://doi.org/10.1186/s13068-017-0945-3.

Terrenoire, E., Hauglustaine, D.A., Gasser, T., Penanhoat, O., 2019. The contribution of carbon dioxide emissions from the aviation sector to future climate change. Environ. Res. Lett. 14 https://doi.org/10.1088/1748-9326/ab3086.

Turton, R., Bailie, R.C., Whiting, W.B., Shaeiwitz, J.A., Bhattacharyya, D., 2012. Analysis, Synthesis, and Design of Chemical Processes, fourth ed. Choice Reviews Online. Pearson. https://doi.org/10.5860/choice.36-0974.

Ukaew, S., Shi, R., Lee, J.H., Archer, D.W., Pearlson, M., Lewis, K.C., Bregni, L., Shonnard, D.R., 2016. Full chain life cycle assessment of greenhouse gases and energy demand for canola-derived jet fuel in North Dakota, United States. ACS Sustain. Chem. Eng. 4, 2771–2779. https://doi.org/10.1021/acssuschemeng.6b00276.

Vásquez, M.C., Silva, E.E., Castillo, E.F., 2017. Hydrotreatment of vegetable oils: a review of the technologies and its developments for jet biofuel production. Biomass Bioenergy 105, 197–206. https://doi.org/10.1016/j.biombioe.2017.07.008.

Veriansyah, B., Han, J.Y., Kim, S.K., Hong, S.A., Kim, Y.J., Lim, J.S., Shu, Y.W., Oh, S.G., Kim, J., 2012. Production of renewable diesel by hydroprocessing of soybean oil: effect of catalysts. Fuel 94, 578–585. https://doi.org/10.1016/j.fuel.2011.10.057.

Vivadinar, A.H., Purwanto, W.W., 2021. Techno-enviro-economic study of hydrogenated vegetable oil production from crude palm oil and renewable hydrogen. IOP Conf. Ser. Mater. Sci. Eng. 1143, 012045 https://doi.org/10.1088/1757-899x/1143/1/012045.

Wang, W.C., 2016. Techno-economic analysis of a bio-refinery process for producing Hydro-processed Renewable Jet fuel from Jatropha. Renew. Energy 95, 63–73. https://doi.org/10.1016/j.renene.2016.03.107.

Wei, H., Liu, W., Chen, X., Yang, Q., Li, J., Chen, H., 2019. Renewable bio-jet fuel production for aviation: a review. Fuel 254. https://doi.org/10.1016/j.fuel.2019.06.007.

Yu, M., Wang, K., Vredenburg, H., 2021. Insights into low-carbon hydrogen production methods: green, blue and aqua hydrogen. Int. J. Hydrogen Energy 46, 21261–21273. https://doi.org/10.1016/j.ijhydene.2021.04.016.

Yukesh Kannah, R., Kavitha, S., Preethi Parthiba Karthikeyan, O., Kumar, G., Dai-Viet, N. V., Rajesh Banu, J., 2021. Techno-economic assessment of various hydrogen production methods – a review. Bioresour. Technol. https://doi.org/10.1016/j.biortech.2020.124175.

Zech, K.M., Dietrich, S., Reichmuth, M., Weindorf, W., Müller-Langer, F., 2018. Techno-economic assessment of a renewable bio-jet-fuel production using power-to-gas. Appl. Energy 231, 997–1006. https://doi.org/10.1016/j.apenergy.2018.09.169.

Zhang, H., Wang, L., Van herle, J., Maréchal, F., Desideri, U., 2020. Techno-economic comparison of green ammonia production processes. Appl. Energy 259, 114135. https://doi.org/10.1016/j.apenergy.2019.114135.

Zhong, H., Jiang, C., Zhong, X., Wang, J., Jin, B., Yao, G., Luo, L., Jin, F., 2019. Non-precious metal catalyst, highly efficient deoxygenation of fatty acids to alkanes with in situ hydrogen from water. J. Clean. Prod. 209, 1228–1234. https://doi.org/10.1016/j.jclepro.2018.10.318.

Zhou, Y., Searle, S., 2022. Cost of Renewable Hydrogen Produced Onsite at Hydrogen Refueling Stations in Europe. ICCT White Pap.

Zhu, Y., Albrecht, K.O., Elliott, D.C., Hallen, R.T., Jones, S.B., 2013. Development of hydrothermal liquefaction and upgrading technologies for lipid-extracted algae conversion to liquid fuels. ALGAL 2, 455–464. https://doi.org/10.1016/j.algal.2013.07.003.

Zoppi, G., Pipitone, G., Gruber, H., Weber, G., Reichhold, A., Pirone, R., Bensaid, S., 2021. Aqueous phase reforming of pilot-scale Fischer-Tropsch water effluent for sustainable hydrogen production. Catal. Today 367, 239–247. https://doi.org/10.1016/j.cattod.2020.04.024.

Zoppi, G., Tito, E., Bianco, I., Pipitone, G., Pirone, R., Bensaid, S., 2023. Life cycle assessment of the biofuel production from lignocellulosic biomass in a hydrothermal liquefaction – aqueous phase reforming integrated biorefinery. Renew. Energy 206, 375–385. https://doi.org/10.1016/j.renene.2023.02.011.